


Research Article

Study of Displacement Characteristics of Fire Flooding in Different Viscosity Heavy Oil Reservoirs

Bingyan Liu,¹ Jinzhong Liang,¹ Fang Zhao,² Tong Liu,² Zongyao Qi,² Fengchao Liu,¹ and Pengcheng Liu ³

¹Beijing Techvista Scientific Co., Ltd., Beijing 100083, China

²State Key Laboratory of Enhanced Oil Recovery, Research Institute of Petroleum Exploration and Development, PetroChina, Beijing 100083, China

³School of Energy Resources, China University of Geosciences, Beijing 100083, China

Correspondence should be addressed to Pengcheng Liu; liupengcheng8883@sohu.com

Received 26 August 2021; Accepted 10 November 2021; Published 23 November 2021

Academic Editor: Tengfei Wang

Copyright © 2021 Bingyan Liu et al. This is an open access article distributed under the Creative Commons Attribution License, which permits unrestricted use, distribution, and reproduction in any medium, provided the original work is properly cited.

A field test in the Xinjiang oilfield in China shows that the viscosity of heavy oil has a certain influence on the combustion dynamics and injection-production performance of fire flooding. The experiment in this study uses a one-dimensional combustion tube to study the temperature, gas composition, and air injection pressure and the production performance of the fire flooding of heavy oil with different viscosities. The results show that the oil viscosities of 1180–22500 mPa·s can achieve stable combustion, and the O₂ content of the gas produced during the stable combustion stage is <0.5%. The higher the viscosity of the heavy oil, the higher the temperature in the burned zone and the smaller the range of the temperature increase in the unburned zone. The air injection pressure will increase rapidly until a stable seepage channel is formed, and then, it will drop to a level close to the formation pressure. High-viscosity heavy oil requires a higher air injection pressure and will remain in the high-pressure stage for a longer period of time. Low-viscosity heavy oil has a low water cut in the early stage of fire flooding, a large oil production rate, and a low and stable air-oil ratio. The water cut of high-viscosity heavy oil increases rapidly in the early stage of fire flooding and then decreases gradually, so a good air-oil ratio can only be obtained in the middle and late stages of fire flooding. Thus, fire flooding may be more suitable for application in common heavy oil and some extra heavy oil reservoirs with lower viscosities.

1. Introduction

Fire flooding is an important method of thermal recovery of heavy oil. It is characterized by a wide reservoir adaptability, sufficient material source, low cost, and high recovery [1]. A large number of field tests and industrial applications have been carried out in Romania, the United States, Canada, India, and other countries [2–4]. The Xinjiang, Shengli, and Liaohe oilfields in China are also conducting fire flooding field tests [5, 6]. Most heavy oil reservoirs in China are sandstone reservoirs with loose cementation, which usually have a high porosity and high permeability. The physical properties of the reservoir are generally not the main constraints in fire flooding development. The main constraint in fire flooding is the viscosity of the heavy oil [7–15]. Unlike

most other countries that conduct fire flooding in reservoirs with formation oil viscosities of less than 5000 mPa·s, the viscosity of the heavy oil in some fire flooding test areas in China can reach 20000 mPa·s. Normal fire flooding production can also be achieved, but the effective time of the surrounding production wells is delayed by 4–6 months [7, 16]. This shows that the viscosity of heavy oil has a certain impact on the combustion dynamics and the injection-production parameters of fire flooding, which leads to high risk and difficulty to grasp the economy of high-viscosity heavy oil fire flooding [17]. The goals of this study were to conduct one-dimensional combustion tube tests using heavy oil with different viscosities and to clarify the influence of the viscosity on the temperature, gas composition, air injection pressure, and production parameters of fire flooding in

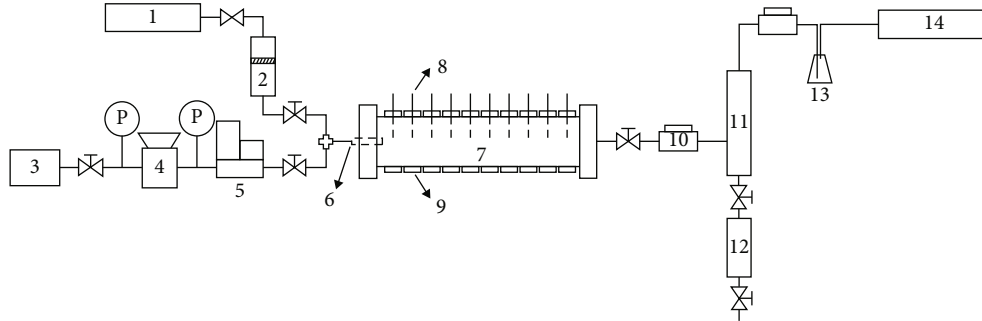


FIGURE 1: Schematic diagram of the combustion tube experimental platform. 1: constant-flux pump; 2: piston container; 3: air source; 4: pressure regulating valve; 5: gas mass flowmeter; 6: igniter; 7: combustion tube; 8: temperature sensor; 9: heating tile; 10: back pressure; 11: first separator; 12: second separator; 13: gas drying bottle; 14: gas component detector.

order to provide a basis for the formulation of a high-viscosity oil reservoir fire flooding plan and the construction of supporting oilfield facilities.

2. Experiments

2.1. Experimental Apparatus. The experiments in this study were conducted using an experimental platform, which can withstand high temperatures and high pressures. The platform is primarily composed of an injection system, a one-dimensional combustion tube, a data acquisition control system, and an output system (Figure 1).

It can monitor the combustion temperature, composition of the gas produced, flow and composition of the liquid produced, and other parameters during the combustion process. There are 16 core temperature sensors evenly distributed in the center of the combustion tube, and 16 wall temperature sensors and heating tiles are evenly distributed on the outside of the combustion tube wall. Therefore, the temperature of the combustion tube wall can be adjusted in real time according to the core temperature, thereby eliminating the temperature difference between the sand pack and the external environment, realizing pseudoadiabatic conditions and accurately simulating the nonisothermal displacement process. The length of the combustion tube is 115 cm, the inner diameter is 5 cm, the volume is 2256 mL, the maximum temperature resistance is 650°C, and the maximum pressure resistance is 15 MPa. The width of each heating tile is 7 cm. The monitoring components of the produced gas are O_2 , CO_2 , and CO .

2.2. Experiment Methods

2.2.1. Experimental Material. Four types of heavy oil were selected, and the viscosity–temperature curves measured after dehydration are shown in Figure 2. The oil sample and reservoir information are presented in Table 1.

2.2.2. Preignition. After filling the combustion tube model with 80–100 mesh quartz sand at room temperature, the model was evacuated and saturated with formation water. Then, the model was heated to 50°C to saturate the oil and achieve the initial oil and water saturations. The procedure was as follows. (1) The output end of the combustion tube model was connected to the vacuum pump, and the injection

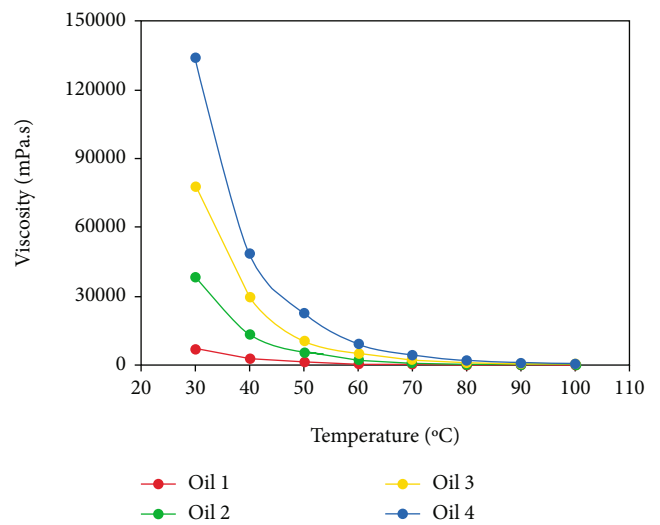


FIGURE 2: Viscosity–temperature curves.

end valve was closed. The vacuum pump was turned on until the degree of vacuum was below 10 Pa. Then, the output end valve was closed, the injection end was connected to the prepared formation water, and the injection end valve was opened so that formation water was automatically sucked into the combustion tube model. (2) The injection end of the model was connected to the pump, and the formation water was injected at a flow rate of 20 mL/min until the output end continuously emitted water and no bubbles flowed out. The volumes of the formation water injected and produced were measured, and the porosity was calculated. (3) The model was heated to 50°C, then heavy oil was injected at a flow rate of 5 mL/min to displace the saturated formation water until no more water was produced. The volumes of the injected and produced heavy oil and the produced water were measured, and the initial oil saturation was calculated. (4) The model was left to stand for 24 hours and prepared for ignition.

The experimental parameters of the four sets of experiments are presented in Table 2.

2.2.3. Ignition and Burning. First, the heating tiles were turned on to heat the combustion tube to 50°C, and the back

TABLE 1: Oil sample and reservoir information.

Oil number	Oilfield	Trap type	Sedimentary facies	Viscosity at 50°C (mPa·s)	Density (g/m ³)
1	Liaohe Shuguang	Monocline	Fan delta front	1180	0.931
2	Xinjing Jiuli	Anticline	Braided channel delta	5483	0.94
3	Tuha Lukeqin	Monocline	Lacustrine fades	10486	0.952
4	Xinjiang z18	Monocline	Channel microfacies	22500	0.975

TABLE 2: Experimental parameters.

Test number	Oil viscosity at 50°C (mPa·s)	Porosity (%)	Initial oil saturation (%)
1	1180	43.32	82.69
2	5483	42.87	83.15
3	10486	41.59	84.26
4	22500	42.03	86.10

pressure at the output end of the model was set to 2 MPa. When the overall temperature of the combustion tube reached 50°C, the igniter was turned on and the igniter temperature was set to 500°C. When the igniter temperature reached 500°C, air was injected into the combustion tube at a rate of 0.7 L/min, and the ventilation intensity of the air was 21.4 m³/(m²·h).

During the experiment, the temperature change at the core temperature sensors of the combustion tube was recorded. When the temperature of each sensor reached the peak, the valve between the first and second separators was opened, the production liquid in the first separator was released into the second separator, and the valve was closed. Finally, the valve on the output end of the secondary separator was opened to collect the produced liquid. This process ensured that the produced gas in the primary separator was continuously collected during the experiment, and the gas composition could be detected by the online gas composition analyzer and was not affected by the outside air.

3. Results and Discussion

3.1. Temperature. The combustion temperature parameters of the four sets of experiments are presented in Table 3. Because the end surface of the model tube was affected by the igniter and the heat dissipation of the flange, the temperature change near the end surface was different from the temperature change during stable combustion. In order to better analyze the combustion parameters during steady combustion, the combustion data between the moment when temperature sensor 4 reached its peak and the moment when temperature sensor 13 reached its peak were analyzed, and the results are shown in Table 4. It was found that under the same experimental conditions, the viscosity of the heavy oil directly affects the combustion front velocity and peak temperature during fire flooding. The higher the viscosity of the heavy oil is, the lower the combustion front velocity is and the higher the peak temperature is. This is because the fuel in the fire flooding process is mainly coke

produced by the cracking of the heavy components of the oil. Oil with a higher viscosity contains more heavy components, and more heavy components are involved in the reaction during combustion to produce more fire flooding fuel. More fuel is consumed and more heat is released. Therefore, the higher the viscosity of the oil is, the higher the peak temperature of the fire flooding is and the higher the fuel consumption is [18–20].

The temperature distribution curves for the combustion tube when sensor 8 reached the peak temperature are shown in Figure 3. As can be seen, when the combustion front advanced to the same distance, the higher the viscosity of the heavy oil was, the higher the temperature in the burned zone was and the smaller the range of the temperature increase in the unburned zone was.

This indicates that during the experiment with low-viscosity oil, more heat was transferred into the unburned zone. Moreover, the range of the unburned zone in which the temperature increase exceeded 50°C was less than 28 cm (width of four heating tiles) in all four sets of experiments. This suggests that while the viscosity of the heavy oil near the combustion front decreased significantly at high temperatures during fire flooding, the temperature of most of the remaining heavy oil did not increase much. Thus, the high temperature viscosity reduction mechanism of fire flooding only has a significant effect on the oil near the combustion front. A large pressure difference is still needed to place the oil far from the combustion front flow.

Figure 4 shows the temperature change curves of sensor 8 for the different experiments. Before the combustion front reaches the temperature measurement point, it mainly relies on heat transfer to increase the temperature, and the temperature rises slowly. After the combustion front advances to the area where the temperature measurement point is located, the heavy oil around the measurement point burns and generates heat, and the temperature at the measurement point increases rapidly. When the combustion front leaves the temperature measurement point, the temperature drops rapidly for a period of time, and then, it drops slowly. There is a clear boundary between the heat transfer heating stage and the combustion heating stage. The experiment with low-viscosity heavy oil entered the combustion stage at a lower temperature, and the experiment with high-viscosity oil needed to reach a higher temperature before it started to burn.

3.2. Gas Component. An on-line gas component detector was used to analyze the gas components produced during the experiments, and the average gas compositions in the stable combustion stage are reported in Table 5. After the

TABLE 3: Combustion temperature parameters.

Sensor number	Distance from injection end (cm)	Test 1		Test 2		Test 3		Test 4	
		Peak temperature (°C)	Time (h)	Peak temperature (°C)	Time (h)	Peak temperature (°C)	Time (h)	Peak temperature (°C)	Time (h)
1	3.59	539	9.20	541	9.44	552	9.81	559	10.42
2	10.78	464	33.55	472	35.18	483	37.28	512	41.79
3	17.97	422	57.33	438	62.69	471	65.29	493	71.44
4	25.16	401	82.34	426	85.39	463	93.21	485	102.20
5	32.34	418	109.22	435	112.25	468	123.64	488	134.33
6	39.53	411	133.29	437	140.01	459	147.94	476	161.57
7	46.72	413	158.74	429	166.44	457	176.23	481	195.96
8	53.91	407	180.74	439	189.75	466	204.55	478	224.94
9	61.09	403	205.37	441	214.89	460	233.41	479	255.48
10	68.28	409	230.78	433	242.62	471	260.00	483	283.75
11	75.47	416	257.39	443	269.93	464	289.75	475	315.44
12	82.66	408	280.34	430	294.09	456	317.09	479	345.32
13	89.84	410	306.73	428	321.15	462	344.66	468	377.63
14	97.03	408	328.91	433	343.94	466	371.58	472	407.55
15	104.22	405	354.00	425	370.79	451	401.25	463	439.69
16	111.41	387	380.03	403	397.45	433	429.30	445	469.28

TABLE 4: The combustion parameters during steady combustion.

Test number	Oil viscosity at 50°C (mPa·s)	Time (min)	Combustion front velocity (mm/h)	Average peak temperature (°C)
1	1180	224.40	172.96	410
2	5483	235.76	164.63	434
3	10486	251.45	154.35	463
4	22500	275.43	140.92	479

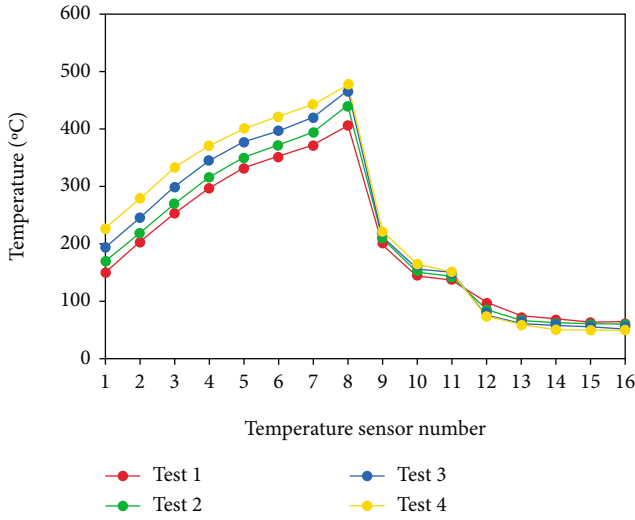


FIGURE 3: Temperature distribution curves when sensor 8 reached the peak.

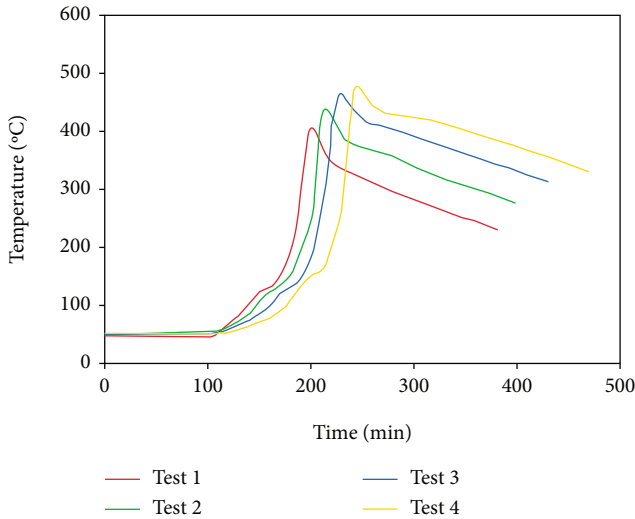


FIGURE 4: Temperature curves for sensor 8.

combustion started, the O₂ content of the four groups of experiments quickly dropped below 0.5%, and the CO₂ content quickly rose to about 14%. The gas produced in the experiment with the high-viscosity oil had a higher CO₂ concentration and lower O₂ and CO concentrations. The difference in the produced gas may not be as obvious in oil-fields due to the long distance between the injection well and

TABLE 5: Average gas components in the stable combustion stage.

Test number	Oil viscosity at 50°C (mPa·s)	O ₂ (%)	CO ₂ (%)	CO (%)
1	1180	0.31	13.38	3.62
2	5483	0.25	13.92	2.59
3	10486	0.22	14.8	1.64
4	22500	0.23	15.54	1.18

production wells [21–23]. However, the O₂ content will always remain within a safe range if combustion can be maintained.

3.3. Injection Pressure. The changes in the air injection pressure with time for the four groups of experiments are shown in Figure 5. The air injection pressure increased rapidly after the start of the experiments. The higher the viscosity of the heavy oil was, the worse the mobility in the formation was, and a higher pressure difference was required for the oil to flow. The injection-production pressure difference more than 8 MPa. After the injection pressure reached the peak, it was maintained for a period of time until the flue gas produced by the combustion advanced to the output end of the model. After a stable seepage channel was formed, the pressure dropped rapidly, and then, the injection pressure remained close to the back pressure. The experiment with lower viscosity oil quickly entered the pressure drop stage, but the high-viscosity experiments required a longer period of high-pressure gas injection. This is because the volume of air under high pressure is reduced, so under standard conditions, more air is needed to form a stable seepage channel. Even after the formation of the seepage channel, the injection pressure of the experiment with high-viscosity oil was greater than that of the experiment with low-viscosity oil. Therefore, high-viscosity fire flooding has higher requirements regarding the performance and stability of the air compressor.

3.4. Production Performance. The output liquid collected during the experiment was weighed and dehydrated, and the quality of the heavy oil and water was measured to obtain the production performance of the combustion tube experiment [24]. The water cut curves are shown in Figure 6, and the flooding efficiency curves are shown in Figure 7. The viscosity of the heavy oil had a significant impact on the production performance of the fire flooding. The low-viscosity experiments had a low water cut in the early stage, a high oil production rate, and a faster increase in the oil displacement efficiency. In the early stage of the

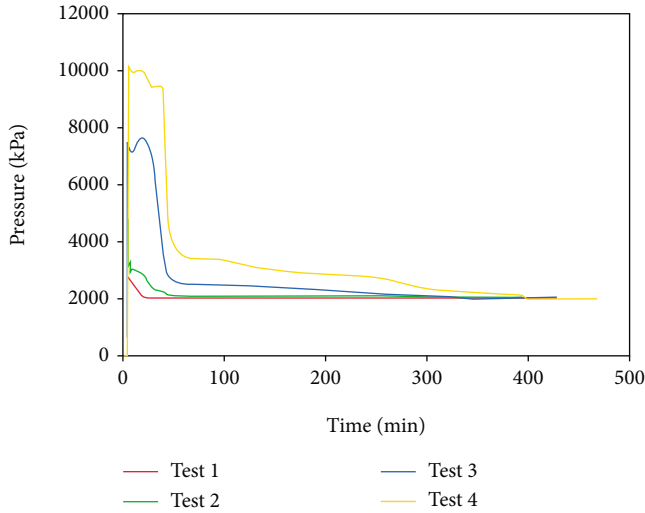


FIGURE 5: Air injection pressure curves.

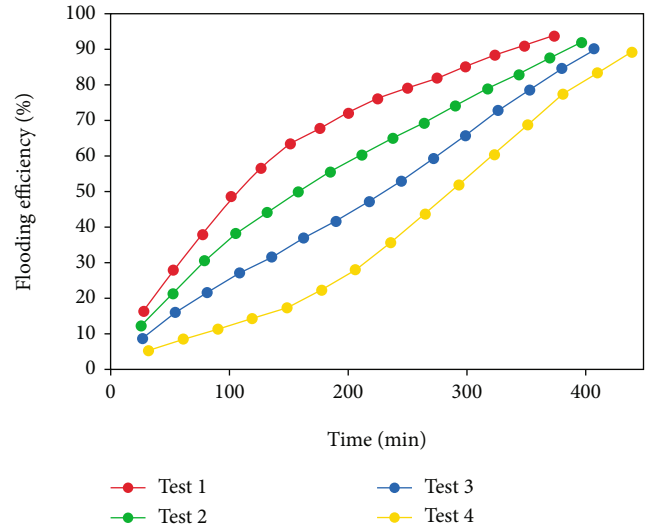


FIGURE 7: Flooding efficiency curves.

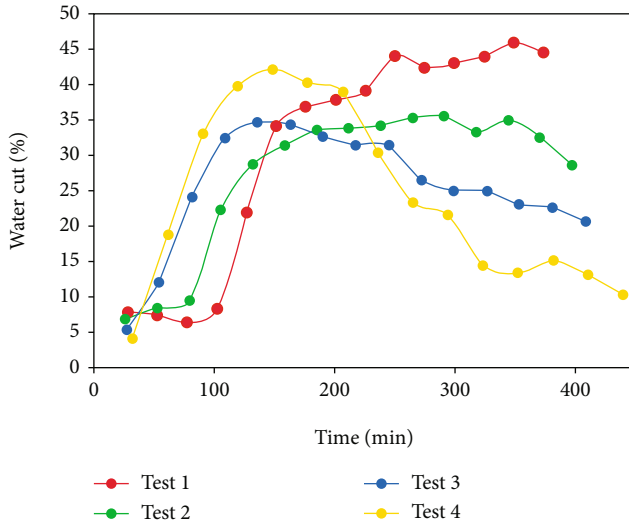


FIGURE 6: Water cut curves.

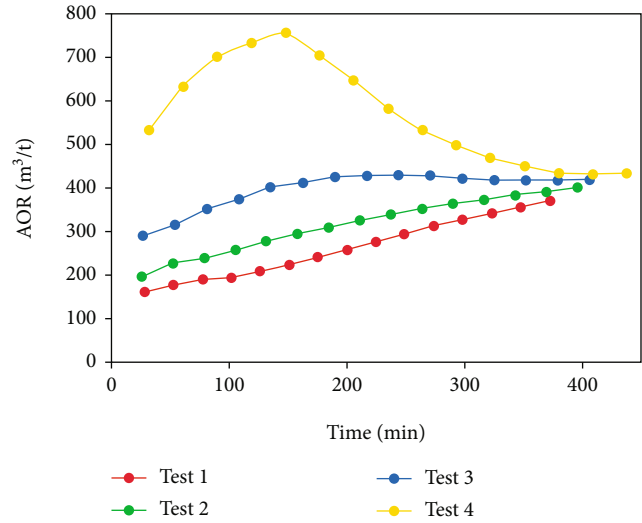


FIGURE 8: AOR curves.

high-viscosity experiment, the oil displacement efficiency increased slowly and the water cut increased rapidly. However, the water cut gradually decreased in the second half of the experiment, and the oil displacement efficiency increased faster. Therefore, low-viscosity heavy oil has higher requirements regarding the dehydration capacity in the middle and late stages of fire flooding. Although the high-viscosity experiment produced less fluid in the early stage, it required a higher dehydration capacity, and the water cut decreased in the later stage. In oilfield development, it is necessary to pay attention to the influence of viscosity on the production performance and to reasonably allocate and construct crude oil treatment facilities.

Injecting compressed air is the main expense of fire flooding, so the air-oil ratio is an important parameter for evaluating the economic benefits of fire flooding in oilfield applications. The cumulative air-oil ratio (AOR) curves of the four groups of experiments are shown in Figure 8. The

lower the viscosity of the heavy oil was, the lower the air-oil ratio was. The fluidity of the crude oil with a lower viscosity increased further under the action of the flue gas produced by the combustion, so a better output and AOR were obtained in the early stage of the experiment. The heavy oil with a higher viscosity could not obtain a good production under only the action of the flue gas, and it required the heat generated by the combustion to reduce the viscosity. Therefore, a better AOR was gradually obtained as the combustion front advanced in the middle and late stages of the experiment. From the perspective of the air-oil ratio, the economic benefits of fire flooding of heavy oil with a lower viscosity are more stable, while fire flooding of heavy oil with a higher viscosity cannot obtain good economic benefits at the beginning of fire flooding. Therefore, fire flooding may be more suitable for application in common heavy oil and some extra heavy oil reservoirs with lower viscosities.

4. Conclusions

- (1) According to the temperature and gas composition data for the combustion tube experiments, it was found that heavy oil with a viscosity of 1180–22500 mPa·s at 50°C can maintain a stable ignition and combustion front. The higher the viscosity of the heavy oil, the more fuel will be involved in the combustion reaction, which will also result in a higher peak temperature and longer experimental time
- (2) The gas produced in the experiment with high-viscosity oil had a higher CO₂ concentration and lower O₂ and CO concentrations. The difference in the gas composition may not be as obvious in oil-fields due to the long distance between the injection well and production well. However, the O₂ content will always remain within a safe range if combustion can be maintained
- (3) After the fire flooding begins, the air injection pressure rises rapidly, a high pressure is maintained for a period of time, and then, the pressure gradually drops to a level close to the formation pressure. The higher the viscosity of the heavy oil, the greater the pressure and the longer it will be maintained for in the high-pressure stage
- (4) The viscosity of heavy oil has a significant impact on the production performance of fire flooding. As the viscosity of the heavy oil increases, the fluid production in the early period decreases and the water cut increases, which results in an increase in the air–oil ratio in the early stage. Thus, fire flooding may be more suitable for application in common heavy oil and some extra heavy oil reservoirs with lower viscosities

Data Availability

All data used to support the findings of this study are available from the corresponding authors on request.

Conflicts of Interest

The authors declare that there is no conflict of interests regarding the publication of this paper.

Acknowledgments

This study was supported by the National Natural Science Foundation of China (No. 51774256). The authors would like to thank the Key Laboratory of Heavy Oil Recovery, CNPC, for the technical support.

References

- [1] S. Yuan, H. Jiang, F. Yang, Y. Shi, Y. Bai, and K. Du, “Research on characteristics of fire flooding zones based on core analysis,” *Journal of Petroleum Science and Engineering*, vol. 170, pp. 607–610, 2018.
- [2] A. Panait-Patica, D. Serban, N. Ilie, L. Pavel, and N. Barsan, “Suplacu de Barcau field—a case history of a successful in-situ combustion exploitation,” in *SPE Europe/EAGE Annual Conference and Exhibition*, Vienna, Austria, 2006.
- [3] S. Roychaudhury, N. S. Rao, S. K. Sinha et al., “Extension of in-situ combustion process from pilot to semi-commercial stage in heavy oil field of Balol,” in *International Thermal Operations and Heavy Oil Symposium*, Bakersfield, California, 1997.
- [4] D. Adabala, S. P. Ray, and P. K. Gupta, “In-situ combustion technique to enhance heavy oil recovery at Mehsana, ONGC—a success story,” in *SPE Middle East Oil and Gas Show and Conference*, Manama, Bahrain, 2007.
- [5] X. Zhang, W. Guan, C. Diao, and C. Xi, “Evaluation of recovery effect in Hongqian-1 wellblock by in-situ combustion process in Xinjiang oilfield,” *Xinjiang Petroleum Geology*, vol. 36, no. 4, pp. 465–469, 2015.
- [6] Y. Liu and S. Hu, “Production performance evaluation of fire flooding in Gao 3-6-18 block,” *Journal of Yangtze University: Natural Science Edition: Science & Engineering*, vol. 6, no. 1, pp. 52–56, 2009.
- [7] W. Guan, X. Zhang, C. Xi et al., “Displacement characteristics and well pattern selection of vertical-well fire flooding in heavy oil reservoirs,” *Acta Petrolei Sinica*, vol. 38, no. 8, p. 935, 2017.
- [8] J. Liang, B. Wang, W. Guan, P. Hou, T. Peng, and L. Miao, “Technology and field test of cyclic in situ combustion in heavy oil reservoir,” *Acta Petrolei Sinica*, vol. 38, no. 3, pp. 324–332, 2017.
- [9] Y. F. Chen, W. F. Pu, X. L. Liu, Y. B. Li, M. A. Varfolomeev, and J. Hui, “A preliminary feasibility analysis of in situ combustion in a deep fractured- cave carbonate heavy oil reservoir,” *Journal of Petroleum Science and Engineering*, vol. 174, pp. 446–455, 2019.
- [10] Z. Yuan, P. Liu, S. Zhang, Y. Jiao, and X. Li, “Experimental study and numerical simulation of a solvent-assisted start-up for SAGD wells in heavy oil reservoirs,” *Journal of Petroleum Science and Engineering*, vol. 154, pp. 521–527, 2017.
- [11] P. Liu, W. Li, and D. Shen, “Experimental study and pilot test of urea- and urea-and-foam-assisted steam flooding in heavy oil reservoirs,” *Journal of Petroleum Science and Engineering*, vol. 135, pp. 291–298, 2015.
- [12] Z. Yuan, P. Liu, S. Zhang, X. Li, L. Shi, and R. Jin, “Experimental study and numerical simulation of nitrogen-assisted SAGD in developing heavy oil reservoirs,” *Journal of Petroleum Science and Engineering*, vol. 162, pp. 325–332, 2018.
- [13] Z. Xu, X. Zhang, Z. Cao et al., “Experimental investigation and numerical simulation of dynamic characteristics for multithermal fluid-assisted SAGD in extraheavy oil reservoir,” *Lithosphere*, vol. 2021, no. Special 1, article 8369713, 2021.
- [14] D. Ji, M. Dong, and Z. Chen, “Analysis of steam-solvent-bitumen phase behavior and solvent mass transfer for improving the performance of the ES-SAGD process,” *Journal of Petroleum Science and Engineering*, vol. 133, pp. 826–837, 2015.
- [15] D. Ji, S. Yang, H. Zhong, M. Dong, Z. Chen, and L. Zhong, “Re-examination of fingering in SAGD and ES-SAGD,” in *SPE Canada Heavy Oil Technical Conference*, Calgary, Alberta, Canada, 2016.
- [16] M. Wang, S. Wang, and S. Huang, *Thermal Flooding Technology of In-Situ Combustion*, Petroleum University Press, Dongying, 1998.

- [17] Q. Xu, H. Jiang, C. Zan et al., “Coke formation and coupled effects on pore structure and permeability change during crude oil in situ combustion,” *Energy & Fuels*, vol. 30, no. 2, pp. 933–942, 2016.
- [18] S. Zhao, W. Pu, B. Sun, F. Gu, and L. Wang, “Comparative evaluation on the thermal behaviors and kinetics of combustion of heavy crude oil and its SARA fractions,” *Fuel*, vol. 239, pp. 117–125, 2019.
- [19] J. D. Alexander, W. L. Martin, and J. N. Dew, “Factors affecting fuel availability and composition during in situ combustion,” *Journal of Petroleum Technology*, vol. 14, no. 10, pp. 1154–1164, 1962.
- [20] N. P. Freitag, “Chemical-reaction mechanisms that govern oxidation rates during in-situ combustion and high-pressure air injection,” *SPE Reservoir Evaluation & Engineering*, vol. 19, no. 4, pp. 645–654, 2016.
- [21] W. Guan, D. Ma, J. Liang, C. Li, C. Xi, and X. Zhang, “Experimental research on thermodynamic characteristics of in-situ combustion zones in heavy oil reservoir,” *Acta Petrolei Sinica*, vol. 31, no. 1, pp. 100–104, 2010.
- [22] W. L. Guan, J. Z. Liang, S. H. Wu, C. F. Xi, and J. H. Huang, “Prediction and controlling method of combustion front in the process of fire-flooding development,” *Journal of Southwest Petroleum University (Science & Technology Edition)*, vol. 33, no. 5, pp. 157–161, 2011.
- [23] D. Aleksandrov, P. Kudryavtsev, and B. Hascakir, “Variations in in-situ combustion performance due to fracture orientation,” *Journal of Petroleum Science and Engineering*, vol. 154, pp. 488–494, 2017.
- [24] J. Tang, W. Guan, J. Liang, H. Jiang, and B. Wang, “Determination on high-temperature oxidation kinetic parameters of heavy oils with thermogravimetric analyzer,” *Acta Petrolei Sinica*, vol. 34, no. 4, pp. 775–779, 2013.